Energy dependence of the imaginary part of the nucleon optical potential

E. Hernández

Instituto de Física, Universidad Nacional Autónoma de México,
Apartado postal 20–364, 01000, México, D.F.

Abstract. The connection between the real and imaginary parts of the nucleon optical potential is explored using the dispersion relations. The potentials are obtained from phenomenological determinations at both negative and positive energies. Particular attention is paid to the radial variation of the potential and its dependence on energy. Twice subtracted dispersion relations are used to obtain the energy variation of the imaginary well depth $W(E)$, using as input the energy variation of the anomaly of the real well depth $V_A(E)$ obtained from phenomenological data. The same dispersion relations are used to derive a simple expression for $W(E)$ as a function of the energy from an expression for the correction to the nucleon's effective mass proposed by G.E. Brown [1]. The energy variation of the anomaly of the real well depth is computed, using as input in the dispersion relations the phenomenologically determined energy variation of the imaginary well depth $W(E)$.

1. Introduction

Some theoretical and empirical developments [1–5] have made possible an understanding of some important effects of the nucleon-nucleus interaction related to the energy dependence of the effective mass of the nucleon in the neighbourhood of the Fermi energy.

Since 1963 [6], it is known that the phenomenologically determined optical potential for nucleons as a function of the energy shows an anomalous behaviour in the vicinity of the Fermi energy [4,6–9].

Theoretical studies made by Bertsch and Kuo [10] show that this effect is due to the dynamical energy dependence appearing in the second and higher order terms of a perturbation expansion of the optical potential. In particular, in second order of perturbation theory the so-colled "polarization" and "correlation" terms show an important energy variation in the neighbourhood of the Fermi energy [2]. The coupling of the single particle modes to the low lying particle-hole configurations of the nuclear core produces a dynamical dependence of the nuclear mean field on the nucleon energy. In the neighbourhood of the Fermi energy, this energy dependence

seems to cancel out partially the energy dependence of the real part of the optical potential coming from the non-locality of the first order Hartree-Fock term. Detailed calculations which include collectivity effects [11–14] confirm the effect predicted by Bertsch and Kuo [10].

On the other hand, studies made from the point of view of the dynamical theory of the collective excitations show that the change of the nucleon's effective mass in the neighbourhood of the Fermi energy E_F makes an important contribution to the strength of the giant resonance [3,15,16].

In a previous paper Bauer *et al.* [4] had studied the energy dependence of the real part of the nucleon optical potential and shown that it can be well described by a quadratic dependence over the whole energy range, with deviations around the Fermi energy that can be attributed to an enhancement of the effective mass as may be seen in Figs. 1 and 2. The overall energy dependence is associated to the non-locality of the potential and the behaviour around the Fermi energy with the higher absorption at these energies.

In the present work, I consider the energy dependence of the imaginary part of the potential making use of the dispersion relations that connect it to the real part. This is done in two ways; firstly using the energy variation already found for the real part [4], and secondly using phenomenological determinations of the imaginary part. Several phenomenological calculations of this type have already been made for finite nuclei and infinite nuclear matter [2,5], and it has been shown that the results are consistent with the phenomenological data for finite nuclei. However, the theory shows that the anomaly around the Fermi energy is more pronounced at lower densities and is thus enhanced in the nuclear surface. The real potential therefore has both volume and surface components, although nearly all phenomenological analysis use the volume form alone. The phenomenological analysis uses either the volume or the surface form for the imaginary part, or sometimes a combination of both forms, and it is found that their relative contributions are not well determined. It is therefore necessary to pay careful attention to the radial variation of both the real and the imaginary potentials when examining the way they are connected by the dispersion relations.

In the next section, the dispersion relations are presented in the form most suitable for the present purpose. In Secc. 3, the relation between the effective mass and the optical potential is discussed in Secc. 4 the results of several analysis of the real part of the potential are used to obtain the imaginary part, and in Secc. 5, several phenomenological determinations of the imaginary part are used to obtain the anomaly of the real part around the Fermi energy. The results are discussed in Secc. 6.

2. Dispersion relations

It is well known that the optical potential is both nonlocal and explicitly energy dependent [17,18]. The analytical properties of the theoretically derived optical potentials come from the causality condition imposed on the Green's function of the

many body system [19]. They allow the derivation of dispersion relations connecting the real part of the optical potential with the imaginary part of the optical potential by means of the Cauchy Theorem

$$\mathcal{V}(r,r';E) = \frac{1}{2\pi i} \int_C \frac{\mathcal{V}(r,r';E')}{(E'-E)} \, dE'. \tag{1}$$

The potential is analytic on the real axis, so the contour may be taken from $-\infty$ to $+\infty$ along that axis.

Since the potential is complex, namely

$$\mathcal{V}(r,r';E) = V(r,r';E) + iW(r,r';E). \tag{2}$$

Eq. (1) can be separated into two dispersion relations connecting the real and imaginary parts of the optical potential, *i.e.*

$$V_A(r,r';E) = \frac{1}{\pi}\mathrm{P}\int_{-\infty}^{+\infty} \frac{W(r,r';E')}{(E'-E)} \, dE' \tag{3}$$

and

$$W(r,r';E) = -\frac{1}{\pi}\mathrm{P}\int_{-\infty}^{+\infty} \frac{V_A(r,r';E')}{(E'-E)} \, dE'. \tag{4}$$

In these equations, P is the principal value and V_A is the anomalous potential defined below in Eq. (7). Although some authors have written the dispersion relations for integration over the energy in the range $0 < E < \infty$, a proper antisymmetrization of the wave function of the many-body system requires that the integration be made from $-\infty$ to ∞. A careful discussion of this important point may be found in the papers by Mahaux and Ngo [2].

In order to guarantee the rapid convergence of the integrals and to avoid normalization problems, it is convenient to make a subtraction. In this way the dispersion relations are written as

$$V_A(r,r';E) - V_A(r,r';E_F) = \frac{(E-E_F)}{\pi}\left(\mathrm{P}\int_{-\infty}^{E_F^-} \frac{W(r,r';E')}{(E'-E)(E'-E_F^-)} dE'\right.$$

$$\left. +\mathrm{P}\int_{E_F^+}^{+\infty} \frac{W(r,r';E')}{(E'-E)(E'-E_F^+)} dE'\right) \tag{5}$$

and

$$W(r,r';E) - W(r,r';E_F) = -\frac{(E-E_F)}{\pi}\left(\mathrm{P}\int_{-\infty}^{E_F^-} \frac{V_A(r,r';E')}{(E'-E)(E'-E_F^-)} dE'\right.$$

$$+P \int_{E_F^+}^{+\infty} \frac{V_A(r, r'; E')}{(E' - E)(E' - E_F^+)} dE' \Bigg) \tag{6}$$

In the case of finite nuclei there is a gap in the integration range from E_F^- to E_F^+ [20,2]. In this work, the value of the Fermi energy used to fix the gap is the average value $E_F = \frac{1}{2}(E_F^- - E_F^+)$.

The real optical potential $V(r, r'; E)$ can be written as an energy independent nonlocal potential $V_{HF}(r, r')$ that may be identified with the local equivalent of the Hartree-Fock potential $V_{HF}(r, E)$ plus a potential $V_A(r, r'; E)$ explicitly energy dependent that represents the anomalous behaviour of the potential around the Fermi surface

$$V(r, r'; E) = V_{HF}(r, r') + V_A(r, r'; E) \tag{7}$$

or

$$V(r, r'; E) - V_{HF}(r, r') = V_A(r, r'; E). \tag{8}$$

A local potential V_L equivalent to the nonlocal $V_A(r, r'; E)$ is obtained following the papers of Bouyssy *et al.* [14] and Perey and Saxon [21]. When $V_L \ll W_L$, the real local potential equivalent to $V_A(r, r'; E)$ is given by

$$\tilde{V}_A(R, (E - V_L)) = \int \exp(ik_L \cdot S) V_A(R, S) dS, \tag{9a}$$

and the imaginary local equivalent potential is

$$\tilde{W}(R, (E - V_L)) = \int \exp(ik_L \cdot S) W(R, S) dS, \tag{9b}$$

where $R = (r + r')/2$, $S = (r - r')$ and k_L is the local wave number defined as

$$k_L^2 = \frac{2m}{\hbar^2}(E - V_L). \tag{10}$$

In this work, I suppose that the effect due to the non-locality of $W(R, S; E)$ and $V_A(R, S; E)$ [22,23,14] produces a smooth energy variation in $\tilde{W}(R, (E - V_L))$ and $\tilde{V}_A(R, (E - V_L))$ which will change only slightly the depth of the potential well and that the dominant energy dependence in $W(R, S; E)$ and $V_A(R, S; E)$ is due to the dynamical dependence on the energy. Therefore, I approximate

$$W(R, S; E) \simeq \delta(S) W(r; E), \tag{11a}$$

$$V_A(R, S; E) \simeq \delta(S) V_A(r; E), \tag{11b}$$

and identify the local optical potential as

$$v(r, E) = V(r, E) + iW(r, E), \tag{12}$$

where the real part is

$$V(r, E) = V_{HF}(r, E) + V_A(r, E), \tag{13}$$

and $V_{HF}(r, E)$ is the local equivalent of the Hartree-Fock potential $V_{HF}(r, r')$.
The dispersion relations, Eqs. (5) and (6), become

$$V_A(r, E) - V_A(r, E_F) = \frac{(E - E_F)}{\pi} \left(P \int_{-\infty}^{E_F^-} \frac{W(r, E')}{(E' - E)(E' - E_F^-)} dE' \right.$$

$$\left. + P \int_{E_F^+}^{+\infty} \frac{W(r, E')}{(E' - E)(E' - E_F^+)} dE' \right) \tag{14}$$

and

$$W(r, E) - W(r, E_F) = -\frac{(E - E_F)}{\pi} \left(P \int_{-\infty}^{E_F^-} \frac{V_A(r, E')}{(E' - E)(E' - E_F^-)} dE' \right.$$

$$\left. + P \int_{E_F^+}^{+\infty} \frac{V_A(r, E')}{(E' - E)(E' - E_F^+)} dE' \right). \tag{15}$$

Since both $V_A(r, E)$ and $W(r, E)$ fall to zero at large energies faster than E^{-1} these integrals are convergent.

For charged particles the electrostatic Coulomb potential must be added to $V(r, r'; E)$ but as it is real and energy independent the subtracted dispersion relations Eqs. (14) and (15) remain unchanged.

3. Relation between the effective mass and the local optical potential

It is convenient to express the real part of the local optical potential $V(r, E)$ in terms of the effective mass m^*, which is usually defined as [2]

$$\frac{m^*}{m} = 1 - \frac{dV(r, E)}{dE}. \tag{16}$$

Using Eq. (13)

$$\frac{m^*}{m}(r, E) = \left(1 - \frac{dV_{HF}(r, E)}{dE} \right) - \frac{dV_A(r, E)}{dE}, \tag{17}$$

the first term in this expression may be calculated starting from the best quadratic fit to the scattering potentials obtained by Bauer *et al.* [4]. It gives, for $r = 0$, a constant value $= 0.6$, which corresponds to the smooth overall energy variation. The second term represents the anomaly around the Fermi energy.

I have done an estimation of the imaginary part of the optical potential $W(0, E)$ starting from the effective mass m^*. Brown *et al.* [1] suggest that the anomaly around the Fermi surface can be represented by a variation of the effective mass of the form

$$\frac{m^*}{m} = 0.64 + 0.36 \left(1 + \frac{|E - E_F|}{2\hbar\omega_0} \right)^{-2}, \tag{18}$$

with $\hbar\omega_0 = 41A^{1/3}$. Making use of Eqs. (17) and (18) we get the correction $V_A(0, E)$ to the real optical potential

$$V_A(0, E) = -0.36 \left(\frac{|E - E_F|}{1 - \frac{|E-E_F|}{2\hbar\omega_0}} \right) \tag{19}$$

This correction to the potential is inserted in the dispersion relation (15) and the integration is carried out analytically giving

$$W_B(0, E) = -\frac{0.72}{\pi} \left(\frac{|E - E_F|}{1 - \left(\frac{|E-E_F|}{2\hbar\omega_0} \right)^2} \right) \ln \left(\frac{|E - E_F|}{2\hbar\omega_0} \right) \tag{20}$$

From Eq. (20), we may observe that $W_B(0, E)$ has a cusp at $E = E_F$, this rather unphysical trait of my result comes from the absolute value $|E - E_F|$ appearing in Brown's approximate expression for the correction to the effective mass, and has no consequence off the very immediate vecinity of E_F. Since $V_A(0, E)$, Eq. (19), is of the volume type, $W_B(0, E)$ is also of the volume type. In the neighbourhood of E_F, $W_B(0, E)$ grows as $(E - E_F)\ln(E - E_F)$ as shown in Fig. 3.

4. Determination of the imaginary potential from the phenomenological real potential

In 1982, Bauer *et al.* [4], studied the energy dependence of the real part of the optical potential for protons on various spherical or nearly spherical nuclei (Fig. 2 of ref. 4). They found that the energy variation of the real part of the optical potential can be described as the sum of two terms: the first one with a quadratic dependence over the energy range -60 MeV $< E < 200$ MeV. The second term, also called the anomaly $V_A(E)$ of the real part of the optical potential, contains the rapid variation of the optical potential observed in the region around the Fermi energy -15 MeV $< E < 15$ MeV. The energy dependence of the anomaly of the real potential $V_A(E)$ was calculated from the correction to the effective mass of the
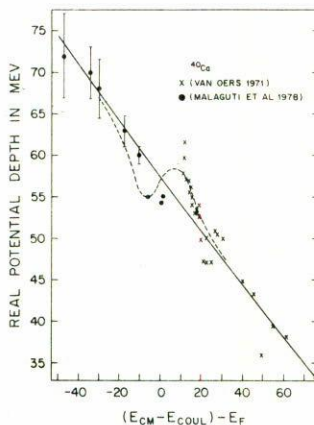
FIGURE 1. Depth of the real central optical potential for protons on ^{40}Ca as a function of proton energy. The points for positive energies refer to potentials from the compilation of van Oers [25], and those for negative energies to potentials fitted to the centroid energies of bound single-particle states [24]. The full line represents the quadratic fit (——) and the dashed line (- - -) the anomaly around the Fermi energy.

nucleons proposed by Brown *et al.* [1]. However, due to the large scatter observed in the data on the real potential depth $V(E)$ for elastic scattering states and to the large error bars of the potential well depth $V(E)$, fitted to the centroid energies of bound single-particle states for many nuclei [24], it is difficult to determine the energy variation of the anomalous potential with acceptable precision. Therefore, in order to determine the imaginary potential, I have decided to concentrate my attention on a single nucleus, namely the phenomenological analysis of protons on ^{40}Ca by van Oers [25], since in this case the scatter observed in the data is rather small.

The imaginary part of the optical potential $W(r, E)$ was obtained from the anomaly of the real part of the optical potential $V_A(r, E)$ and the dispersion relation given in Eq. (15).

The anomaly $V_A(r, E)$ of the real part of the optical potential for ^{40}Ca shown in Fig. 1, was extracted directly from the phenomenological data. According to Eq. (13) the anomaly $V_A(r, E)$ is obtained subtracting from the phenomenological real optical potential $V(r, E)$ the equivalent local Hartree-Fock potential $V_{HF}(r, E)$. The phenomenological real potentials [25], used in the study of the energy dependence are written as
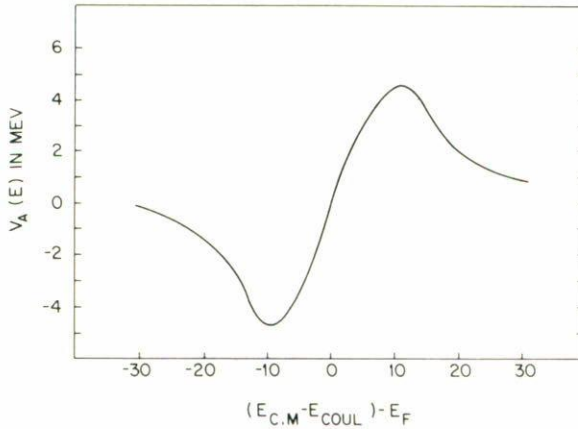
$$V(r, E) = V(E)f(r),$$

FIGURE 2. Depth of volume real correction term for ^{40}Ca as function of energy. The full line represents the anomaly of the real potential $V_A(r, E)$ obtained subtracting the quadratic fit shown in Fig. 1 to the experimentally determined values of the real potential.
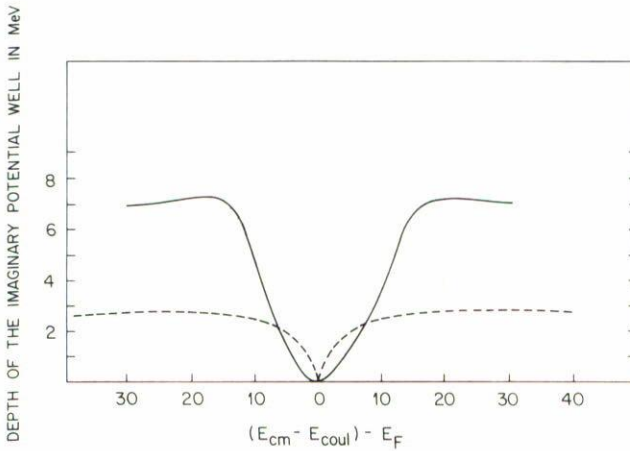

FIGURE 3. Depth of the volume imaginary optical potential for protons on ^{40}Ca, as function of the energy. The curves represents the results of the numerical computation of the twice subtracted dispersion relation (—) and to the calculations of the effective mass using the formula of Brown *et al.* [1] (- - -).

where $f(r)$ is a form factor of the Woods-Saxon type. The depth of the potential well $V(E)$ as a function of the energy is shown in Fig. 1: The real potential $V_{HF}(r, E)$ was determined following the procedure described in the paper of Bauer *et al.* [4], we made a least squares fit of a quadratic form to the experimental points shown in

Nucleus	V_0	α'	β'
^{40}Ca	57.216 ± 2.21	-0.333 ± 0.072	0.00025 ± 0.0002

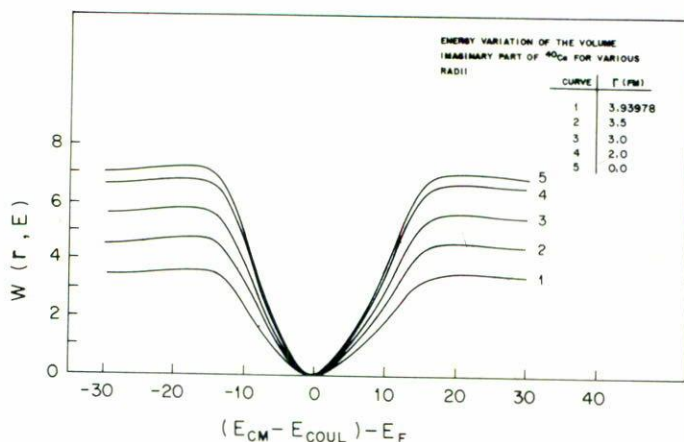TABLE I. Parameters of the best fit to the depth of the potential well as function of energy.

FIGURE 4. The volume imaginary potential for ^{40}Ca as function of the energy. The curves represent the results obtained from the numerical calculation of the twice subtracted dispersion relation, for different values of the nuclear radius.

Fig. 1, excluding those points in the energy range -22 MeV $< \{(E_{\text{c.m.}} - E_{\text{Coul}}) - E_F\} < 22$ MeV. The best-fit values of the parameters are given in Table 1.

The anomaly term $V_A(E)$, of the real part of the optical potential, was calculated from the difference between a curve drawn through the experimental points (dashed-line in Fig. 1) and the quadratic fit (full-line in Fig. 1).

The anomaly $V_A(E)$, shown in Fig. 2, is used as input in the dispersion relation Eq. (15) and I obtain the volume imaginary potential $W(E)$ shown in Fig. 3. The volume imaginary potential obtained from the numerical calculation is a symmetric function of $(E_{\text{c.m.}} - E_{\text{Coul}}) - E_F$. The Coulomb energy E_{Coul}, was computed following the procedure of Giannini *et al.* [26]. The Fermi energy was taken as $E_F = 8.3 \, MeV$. For values of $(E_{\text{c.m.}} - E_{\text{Coul}}) \simeq E_F$ the imaginary potential depth rises with $E = (E_{\text{c.m.}} - E_{\text{Coul}})$ as $(E - E_F)^2$, this behaviour is in agreement with the phenomenological data contained in the compilation by Mahaux and Ngo [2]. The imaginary potential $W(E)$ obtained from the phenomenological data raises to a much larger value than the one obtained from Brown's approximation to the effective mass, as may be seen in Fig. 3. The radial variation of the imaginary potential $W(r, E)$ is shown in Fig. 4 for different values of the nuclear radius R.

5. Phenomenological determination of the imaginary potential

The imaginary potential may be determined in three energy regions from different experimental data. At negative energies $E < E_F$ it is related to the widths Γ of the bound states as determined by measurements of the $(p, 2p)$ and $(e, e'p)$ reactions. Just above E_F, it may be obtained from the S-strength functions and at higher energies from phenomenological optical model analysis of elastic scattering cross-sections. A compilation of data by Mahaux and Ngo [2], shows that the imaginary potential depends parabolically on $|E - E_F|$ around E_F, reaches a maximum around $|E - E_F| = 40$ MeV and thereafter falls. A potential of this form, when inserted into the dispersion relation, gives a real potential in good agreement with the phenomenological determinations.

I have collected a large amount of data, from $(p, 2p)$ and $(e, e'p)$ reactions. However, the scatter of experimental points is so large that it is not possible to determine the energy variation of the imaginary potential univocally. The dispersion of the data may be due to the actual differences in nuclear structure of the various nuclei considered, which affect the imaginary potential more strongly than the real potential. They may also be due to the different form factors used in the phenomenological analysis, and the ambiguities inherent in such analysis.

Therefore, I decided to concentrate my attention on a careful analysis of proton elastic scattering data which was made in terms of a combination of volume and surface imaginary potentials. In particular, the analysis of the data made by van Oers [25], for protons on ^{40}Ca and the analysis made by Thomas and Burge [27], of the elastic scattering of protons on ^{58}Ni. The values of the imaginary well depth determined by these authors are shown in Figs. 5 and 6.

A curve was drown through the points representing values of the imaginary well depth versus energy. The numerical values of $W_v(E)$ and $W_D(E)$ represented by the curve are then used as input in the dispersion relation Eq. (14) to extract the corresponding numerical values of the real potential well depths. In order to perform the numerical integration, it was assumed that the imaginary potential depths as function of the energy are symmetrical around the Fermi energy. The resulting real potentials

$$V_v(r, E) = V_v(E)f(r)$$

$$V_D(r, E) = V_D(E)g(r)$$

where evaluated at the average geometry radius $r = r_W A^{1/3}$. The results are shown in Figs. 7 and 8. At this point, the Woods-Saxon form factors and the derivative Woods-Saxon form factors are $f(r) = \frac{1}{2}$ and $g(r) = 1$. The average geometry radius for ^{40}Ca is $r_W = 1.309$ fm and for ^{58}Ni is given by $r_W = 1.16$ fm. It may be observed that at low energies the surface term V_D is dominant. At higher energies both terms are large but have opposite sign. Adding the two contributions, we obtain the anomaly of the real part $V_A(r, E)$ at $r = r_W A^{1/3}$, which is shown in Figs. 9 and 10. It may be seen that at low energies there is a sharp maximum
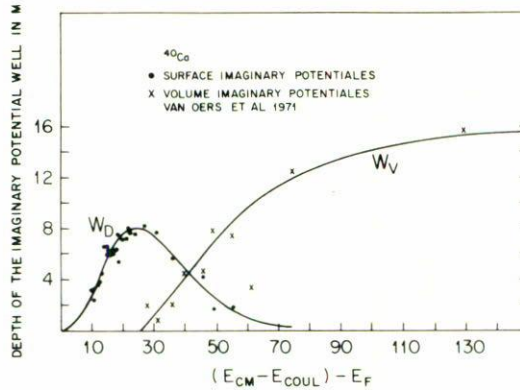
FIGURE 5. Depth of the imaginary optical potential for protons on ^{40}Ca as a function of the energy. The dots ($\cdot$) represent the surface potentials and the crosses ($\times$) the volume potentials, from van Oers [25]. The full line represents an average value of the depth of the imaginary optical potential obtained by interpolating between the values of the imaginary potential well derived from experiment.
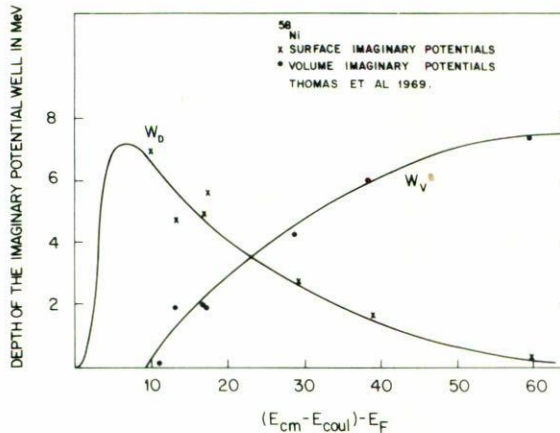

FIGURE 6. Depth of the imaginary optical potential for protons on ^{58}Ni as function of the energy. The dots ($\cdot$) represent the volume potentials and the crosses ($\times$) the surface potentials, from Thomas *et al.* [27]. The full line represents an average value of the depth of the imaginary optical potential obtained by interpolating between the values of the imaginary potential well derived from experiment.

that comes from the surface contribution, at higher energies the curve falls to small negative values. In the case of ^{40}Ca, where the contribution to the correction term $V_A(r, E)$, that comes from the volume component is known in a large energy region
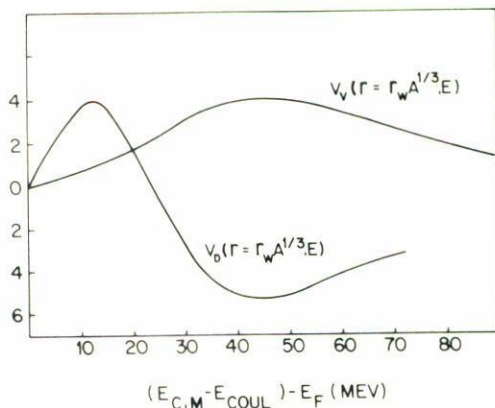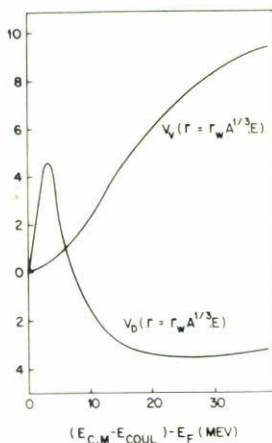
FIGURE 7. The surface correction term $V_D(r = r_W A^{1/3}, E)$ and the volume correction term $V_v(r = r_W A^{1/3}, E)$ of the real part of the optical potential for ^{40}Ca, evaluated at the surface radius, as a function of the energy.

FIGURE 8. The surface correction term $V_D(r = r_W A^{1/3}, E)$ and the volume correction term $V_v(r = r_W A^{1/3}, E)$ of the real part of the optical potential for ^{58}Ni, evaluated at the surface radius, as a function of the energy.

25 MeV $< E <$ 150 MeV, the behaviour of the correction term $V_A(r, E)$ of the real part of the optical potential is better determined than in the case of ^{58}Ni, for energies $E <$ 30 MeV. On the other hand, the average geometry obtained from the phenomenological analysis allows me to show the behaviour of the correction
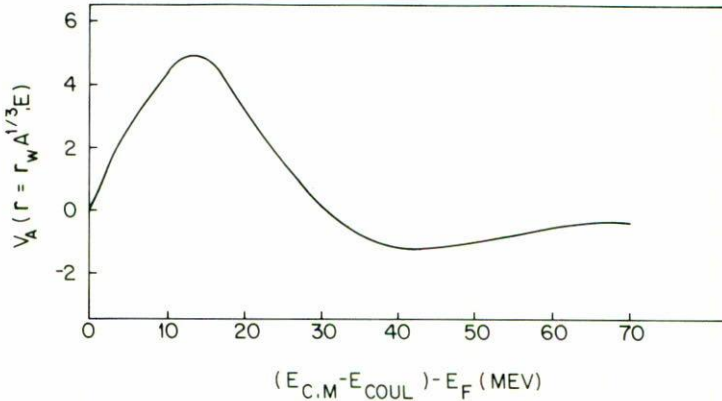
FIGURE 9. Full correction term $V_A(r = r_W A^{1/3}, E)$ to the real optical potential for ^{40}Ca evaluated at the surface radius as a function of the energy.
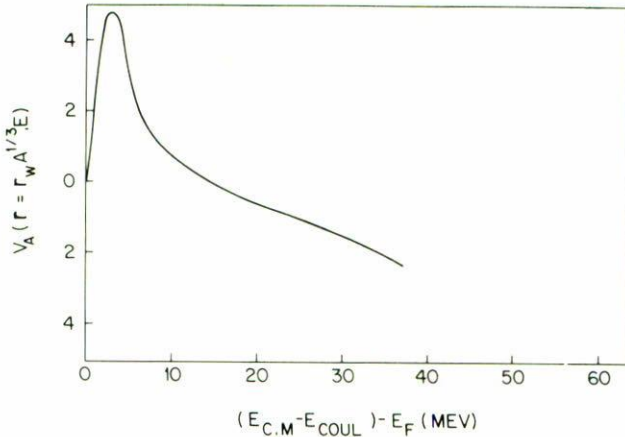

FIGURE 10. Full correction term $V_A(r = r_W A^{1/3}, E)$ to the real optical potential for ^{58}Ni evaluated at the surface radius as a function of the energy.

term $V_A(r, E)$ to the real part of the optical potential for different values of the nuclear radius r, as a function of the energy $(E_{c.m} - E_{Coul}) - E_F$. This behaviour of the correction term $V_A(r, E)$ is shown in Fig. 11. It is clear from this plot that the effect which produces the anomaly on the real part of the optical potential is localized at the surface of the nucleus and therefore it is predominantly a surface effect. At energies around 21 MeV, the correction term $V_A(r, E \simeq 21)$ does not change with r in the interior of the nucleus. At energies lower than 25 MeV, the absorption is mainly a surface effect that goes to zero as we approach the centre of
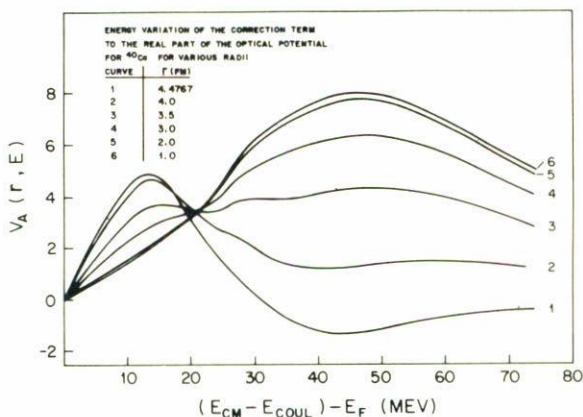
FIGURE 11. Energy variation of the correction term to the real part of the optical potential for ^{40}Ca for various values of the nuclear radius.
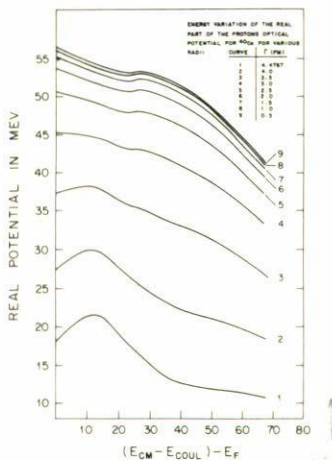

FIGURE 12. Energy variation of the real part of the proton optical potential for ^{40}Ca for various values of the nuclear radius.

the nucleus. At energies larger than 25 MeV a volume absorption effect starts to be important for values of r smaller than 3 fm. At the centre of the nucleus ($r = 0$, $f(r) = 1$, $g(r) = 0$) the contribution to $V_A(0, E)$ obtained from $W(E)$ by means of the dispersion relation is exclusively of the volume type. It raises from zero very slowly to a maximum value around 45 MeV as may be seen in Fig. 11. Since this contribution is important at rather high energies, it is probably not due to the same

effect that produces the anomaly in the effective mass. It probably comes from an enhanced absorption due to the opening of many new channels or giant resonances.

The calculation of the real part of the optical potential as function of the energy, Fig. 12, shows clearly that the anomaly on the neighbourhood of the Fermi energy is produced by surface contributions. For values of the nuclear radius smaller than the surface radius, the anomaly goes to zero and other effect, a volume one, starts to be important.

6. Conclusions

It was found that there is an inconsistency in the determination of the anomaly $V_A(r, E)$ of the real part of the optical potential extracted directly from the phenomenological data, and the anomaly $V_A(r, E)$ calculated using as input in the dispersion relation, Eq. (14), the phenomenological data of the imaginary potential $W(r, E)$. The anomaly of the real optical potential extracted from the phenomenological data is of the volume type, whereas the anomaly $V_A(r, E)$ calculated using the dispersion relations is the sum of two terms: a volume term plus a surface term. This inconsistency in the determination of $V_A(r, E)$ is essentially due to the fact that the phenomenological parametrizations do not take into account the functional dependence of $V_A(r, E)$ on the imaginary potential $W(r, E)$ expressed in the dispersion relations.

The behaviour of the volume imaginary potential obtained inserting in the dispersion relation the phenomenologically determined anomaly of the real potential for ^{40}Ca, is in good agreement with the behaviour observed in the phenomenological data of the compilation of Mahaux and Ngo [2,5].

At positive energies lower than 30 MeV the anomaly $V_A(r, E)$ of the real potential, obtained from the energy variation of the imaginary potential for ^{40}Ca and ^{58}Ni and the dispersion relation Eq. (14), is the sum of a predominantly surface term plus a small volume term.

It is also found that at low energies $(\{E_{c.m} - E_{Coul}\} - E_F) < 40$ MeV the real part of the phenomenological optical potential may be written as the sum of two terms: a volume type term $V_{HF}(r, E)$ with a quadratic dependence on the energy over the whole energy range, and a predominantly surface term, $V_A(r, E)$ that raises from zero at $(E_{c.m} - E_{Coul}) = E_F$ to a maximum values around $E_{c.m} - E_{Coul}) = E_F = 25$ MeV and then falls to small negative values. This surface effect is of the same type as the surface effect found by G.E. Brown *et al.* [1], in the coupling of vibration collective modes to the single particles motion and in the microscopic calculation of Wambach *et al.* [16] and Mahaux and Ngo [2,5]. The parameters of the real surface term are the same as those of the surface absorption.

Acknowledgements

References

1. G.E. Brown, J.S. Dehesa and J. Speth, *Nucl. Phys.* **A330** (1979) 290.
2. C. Mahaux and H. Ngo, *Phys. Lett.* **100B** (1981) 285; C. Mahaux and H. Ngo, *Nucl. Phys.* **A378** (1982) 205.
3. G.E. Brown and Rho Mannque, *Nucl. Phys.* **A372** (1981) 397.
4. M. Bauer, E. Hernández-Saldaña, P.E. Hodgson and J. Quintanilla, *J. Phys.* **G8** (1982) 525.
5. C. Mahaux and R. Sartor, *Nucl. Phys.* **A484** (1988) 205; C.H. Johnson, D.J. Horen and C. Mahaux, *Phys. Rev.* **C36** (1987) 2252; C. Mahaux and R. Sartor, *Nucl. Phys.* **A468** (1987) 193.
6. G.E. Brown, J.H. Gunn and P. Gould, *Nucl. Phys.* **46** (1963) 598.
7. B.L. Cohen and M.A. Ruderman, *Phys. Rev.* **128** (1962) 1474.
8. G.J. Batty and G.W. Greenless, *Nucl. Phys.* **A133** (1969) 673.
9. K. Bear and P.E. Hodgson, *J. Phys.* **G4** (1978) L287.
10. G.F. Bertsch and T.T.S. Kuo, *Nucl. Phys.* **A112** (1968) 104.
11. S. Fantoni, B.L. Friman and V.R. Pandharipande, *Phys. Lett.* **100B** (1981) 89.
12. V. Bernard and N. van Giai, *Nucl. Phys.* **A348** (1980) 75.
13. C.H. Li and V. Klemt, *Nucl. Phys.* **A364** (1981) 93.
14. A. Bouyssy, H. Ngo and N. Vinh Mau, *Nucl. Phys.* **A371** (1981) 173.
15. P.E. Bortignon and R.A. Broglia, *Nucl. Phys.* **A371** (1981) 405.
16. W. Wambach, V.K. Mishra and Li-Chu-Hsia, *Nucl. Phys.* **A380** (1982) 285.
17. H. Feshbach, *Ann. Phys.* **51** (1958) 357.
18. J.S. Bell and E.J. Squires, *Phys. Rev. Lett.* **3** (1959) 96.
19. R. Lipperheide, *Nucl. Phys.* **89** (1966) 97.
20. E.E.H. Gross and R. Lipperheide, *Nucl. Phys.* **A150** (1970) 449.
21. F.G. Perey and G. Saxon, *Phys. Rev.* **28** (1964) 107.
22. R. Lipperheide and A.K. Schmidt, *Nucl. Phys.* **A122** (1968) 65.
23. N. Vinh Mau and A. Bouyssy, *Nucl. Phys.* **A257** (1976) 189.
24. F. Malaguti, A. Uguzzoni, E. Verondini and P.E. Hodgson, *Il Nuovo Cimento* **49** (1979) 412; F. Malaguti, A. Uguzzoni, E. Verondini and P.E. Hodgson, *Nucl. Phys.* **A297** (1978) 287.
25. V.T.H. van Oers, *Phys. Rev.* **C3** (1971) 1550.
26. M.M. Giannini, G. Ricco and A. Zucchiatti, *Ann. Phys.* **124** (1980) 208.
27. G.L. Thomas and E.J. Burge, *Nucl. Phys.* **A128** (1969) 545.

Resumen. La conexión entre la parte real y la parte imaginaria del potencial óptico se explora usando las relaciones de dispersión. Los potenciales se obtienen de determinaciones fenomenológicas a energías positivas y a energías negativas. Especial atención se dedica a la variación radial del potencial y su dependencia con la energía. La variación con la energía de la profundidad del potencial imaginario $W(E)$, se obtiene a partir de la variación con la energía de la anomalía del potencial real $V_A(E)$ mediante el uso de una relación de dispersión substraída. La misma relación de dispersión se usa para derivar una expresión simple para $W(E)$ como función de la energía a partir de una expresión para la corrección a la masa efectiva de los nucleones, propuesta por G.E. Brown [1]. La variación con la energía de la anomalía de la parte real del potencial óptico se calcula usando como información en las relaciones de dispersión la variación con la energía de la profundidad del potencial imaginario $W(E)$, el cual se obtiene de los datos fenomenológicos.